ATTITUDE CONTROL OPTIMIZATION FOR A SMALL-SCALE UNMANNED HELICOPTER

Bernard Mettler and Takeo Kanade
The Robotics Institute
Carnegie Mellon University
Pittsburgh, Pennsylvania

Mark B. Tischler
Army/NASA Rotorcraft Division
Aeroflightdynamics Directorate (AVRDEC)
US Army Aviation and Missile Command
Ames Research Center

William Messner
Departement of Mechanical Engineering
Carnegie Mellon University
Pittsburgh, Pennsylvania

Abstract: This paper presents results from the attitude control optimization for a small-scale helicopter by using an identified model of the vehicle dynamics that explicitly accounts for the coupled rotor/stabilizer/fuselage (r/s/f) dynamics. The accuracy of the model is verified by showing that it successfully predicts the performance of the control system currently used for Carnegie Mellon's autonomous helicopter (baseline controller). Elementary stability analysis shows that the light damping in the coupled r/s/f mode, which is due to the stabilizer bar, limits the performance of the baseline control system. This limitation is compensated by a second order notch filter. The control system is subsequently optimized using the CONDUIT control design framework with a frequency response envelope specification, which allows the attitude control performance to be accurately specified while insuring that the lightly damped r/s/f mode is adequately compensated.

Introduction

The successful application of small-scale autonomous helicopters depends on their level of controllability and flying qualities. The variety of modes under which small-scale autonomous helicopters can be deployed, e.g., from remotely operated to fully autonomous operation, the inherently faster dynamics, and the differences in configuration all contribute to the difficulty of the control design. In order to attain a satisfactory level of performance, a systematic study of their dynamics and the performance requirements is necessary.

Despite the attention that the control problem of small-scale helicopters has received in the past, the current level of control performance is still far less than the potential of the vehicle. Often the performance barely satisfies the requirements for simple applications. The limited performance is typically due to insufficient understanding of the small-scale helicopters' flight dynamics.

For full-size helicopters linear system identification plays an important role in the understanding and modeling of the dynamics. With frequency domain identification methods, such as CIFER (Comprehensive Identification from FrEquency Responses) [1], the key dynamic effects, such as the dynamic coupling between the rotor and the fuselage, can be recognized and then explicitly accounted for in the model.

We derived such models (hover and cruise condition) for the Yamaha R-50 helicopter [2]. The models explicitly account for the characteristics that are relevant in small-scale helicopters such as the stabilizer bar. From the identification modeling process, we were able to understand the particularities of small-scale helicopter dynamics.

The identified dynamic models are now used to understand the control performance requirements of small-scale helicopters and support advanced control design that will aid in exploiting the potential of this special class of vehicles.

This paper shows analysis and control optimization results of the PD control system currently used in our autonomous R-50 helicopter. All results were derived using the identified model. The accuracy of the augmented vehicle dynamics (vehicle dynamics with control system) used for the analysis has been successfully validated against flight test data obtained from closed loop experiments. Stability analysis shows that the stabilizer bar is a major performance limitation for our baseline control system. A notch filter addresses this limitation. To exploit the inherent performance of the compensated system (baseline system with notch filter), we use the Control Designer's Unified Interface (CONDUIT) developed by the Army and NASA [3]. To achieve the desired performance characteristics, we developed a frequency response envelope specification. Using this approach, we can design controllers with

different performance levels. Finally, using Bode stability analysis, we show the impact of the attitude control performance on the helicopter's velocity and position controllability.

Description of the Small-Scale R-50 Helicopter

The Yamaha R-50 helicopter used in the HUAV project at Carnegie Mellon University (CMU) (shown in Table 1) is a commercially available model-scale helicopter originally designed for remotely operated crop-dusting. Because of the adequate payload (50 lb.) and the reliable operation, the R-50 has become the platform of choice for research in autonomous helicopter flight. General physical characteristics of the R-50 are provided in Table 1.

The R-50 uses a two-bladed main rotor with a Bell-Hiller stabilizer bar. The relatively rigid blades are connected to a yoke by means of individual flapping hinges and elastomeric fittings. The yoke itself is attached to the rotor shaft over a teetering hinge in an under-swung configuration. The teetering motion is also restrained by an elastomer damper/spring. This rotor system differs from classical teetering rotors in that it is stiffer and accommodates teetered and separately hinged blade motion.

The Bell-Hiller stabilizer bar is a secondary rotor consisting of a pair of paddles connected to the rotor shaft through an unrestrained teetering hinge. The stabilizer bar receives the same cyclic control input as the main rotor, but it has a slower response than the main blades and is also less sensitive to airspeed and wind gusts due to a smaller blade lock number γ (non-dimensional rotor parameter relating the ratio between aerodynamic and inertia forces). The stabilizer bar flapping motion is used to generate a control augmentation to the main rotor cyclic input. This augmentation is implemented by the Bell mixing mechanism. From a control theoretical point of view, this can be interpreted as a lagged rate (or "pseudo-attitude") feedback in the pitch and roll loops [2,4]. The pseudo-attitude feedback also reduces the response of the aircraft to wind gusts.

Stabilizer bars are common in small-scale helicopters because they display less rotor-induced damping than full scale ones. The stabilizer bar compensates for this deficiency, facilitating the human operation. Rotor-induced damping arises from the tendency of the rotor disc – therefore, of the thrust vector – to lag behind the shaft during pitching or rolling angular motions. This lag, which is proportional to the rotor time constant, produces a moment about the helicopter center of gravity opposite to the rolling or pitching direction and proportional to the rolling or pitching rate. The time constant of a rotor τ is function of the non-dimensional blade lock number γ and the rotor speed Ω ($\tau = 16/\gamma\Omega$). For a rotor scale N (i.e., rotor size is $1/N$-th of the full size rotor diameter) the model-scale helicopter must have a rotor speed that is about $\sqrt{N}$ of the full size helicopter in order to achieve a sufficiently large blade-tip speed (the blade tip speed must be large enough to prevent retreating blade stall, yet not too large to avoid reaching subsonic speed on the advancing side). Therefore, the rotor time constant of a small-scale helicopter is $\sqrt{N}$ (R-50: $\sqrt{5}=2.24$) times smaller than that of a full-scale helicopter, and the rotor induced damping will also be $\sqrt{N}$ smaller. A smaller rotor time constant also means a larger control bandwidth.

Table 1 – R-50 Physical Characteristics

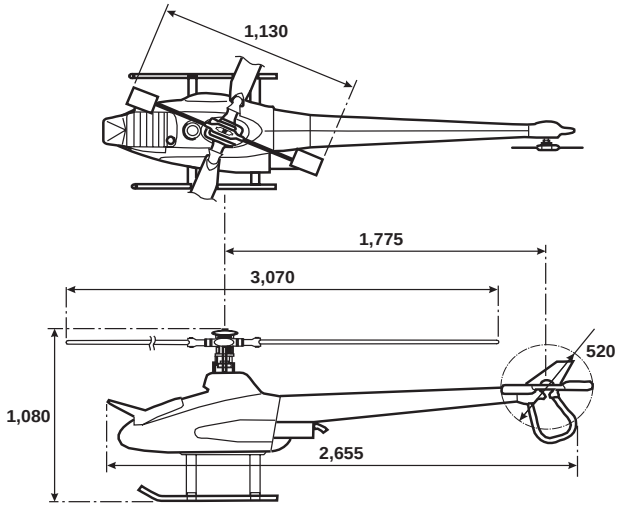

Dimensions	See Figure (in meters)
Rotor speed Tip speed	850 rpm 449 ft/s
Dry weight Instrumented (full payload capacity)	97 lb. 150 lb.
Engine type	Single cylinder, 2-stroke, water cooled
Flight autonomy	30 minutes

Table 2 – State-space model structure of the R-50 with rotor and stabilizer bar equations

$$\begin{bmatrix} \dot{u} \\ \dot{v} \\ \dot{p} \\ \dot{q} \\ \dot{\phi} \\ \dot{\theta} \\ \tau_f \dot{a} \\ \tau_f \dot{b} \\ \dot{w} \\ \dot{r} \\ \dot{r}_{fb} \\ \tau_s \dot{c} \\ \tau_s \dot{d} \end{bmatrix} = \begin{bmatrix} X_u & 0 & 0 & 0 & 0 & -g & X_a & 0 & 0 & 0 & 0 & 0 & 0 \\ 0 & Y_v & 0 & 0 & g & 0 & 0 & Y_b & 0 & 0 & 0 & 0 & 0 \\ L_u & L_v & \mathbf{0} & 0 & 0 & 0 & 0 & L_b & L_w & 0 & 0 & 0 & 0 \\ M_u & M_v & 0 & 0 & 0 & 0 & M_a & 0 & M_w & 0 & 0 & 0 & 0 \\ 0 & 0 & 1 & 0 & 0 & 0 & 0 & 0 & 0 & 0 & 0 & 0 & 0 \\ 0 & 0 & 0 & 1 & 0 & 0 & 0 & 0 & 0 & 0 & 0 & 0 & 0 \\ 0 & 0 & 0 & -\tau_f & 0 & 0 & -1 & A_b & 0 & 0 & 0 & A_c & 0 \\ 0 & 0 & -\tau_f & 0 & 0 & 0 & B_a & -1 & 0 & 0 & 0 & 0 & B_d \\ 0 & 0 & 0 & 0 & 0 & 0 & Z_a & Z_b & Z_w & Z_r & 0 & 0 & 0 \\ 0 & N_v & N_p & 0 & 0 & \mathbf{0} & 0 & 0 & N_w & N_r & N_{rfb} & 0 & 0 \\ 0 & 0 & 0 & 0 & 0 & 0 & 0 & 0 & 0 & K_r & K_{rfb} & 0 & 0 \\ 0 & 0 & 0 & -\tau_s & 0 & 0 & 0 & 0 & 0 & 0 & 0 & -1 & 0 \\ 0 & 0 & -\tau_s & 0 & 0 & 0 & 0 & 0 & 0 & 0 & 0 & 0 & -1 \end{bmatrix} \begin{bmatrix} u \\ v \\ p \\ q \\ \phi \\ \theta \\ a \\ b \\ w \\ r \\ r_{fb} \\ c \\ d \end{bmatrix} + \begin{bmatrix} 0 & 0 & 0 & 0 \\ 0 & 0 & Y_{ped} & 0 \\ 0 & 0 & 0 & 0 \\ 0 & 0 & 0 & M_{col} \\ 0 & 0 & 0 & 0 \\ 0 & 0 & 0 & 0 \\ A_{lat} & A_{lon} & 0 & 0 \\ B_{lat} & B_{lon} & 0 & 0 \\ 0 & 0 & 0 & Z_{col} \\ 0 & 0 & N_{ped} & N_{col} \\ 0 & 0 & 0 & 0 \\ 0 & C_{lon} & 0 & 0 \\ D_{lat} & 0 & 0 & 0 \end{bmatrix} \begin{bmatrix} \delta_{lat} \\ \delta_{lon} \\ \delta_{ped} \\ \delta_{col} \end{bmatrix}$$

Dynamics of the Small-Scale R-50 Helicopter

Identified Dynamic Model

The model of the R-50 dynamics was derived using CIFER frequency domain identification techniques [2]. The modeling using linear frequency identification techniques consists of the following steps: first, flight data is collected using frequency sweep techniques; second, from the flight data the frequency responses for each input-output pairs are computed; third, a parameterized linear model which captures the relevant features of the dynamics is derived using basic helicopter theory [5]. The frequency responses computed from the flight data provide important information about the dynamic characteristics; fourth, the parameters of the linear dynamic model are identified during an optimization process driven by the difference between the computed and predicted frequency responses; last, the fidelity of the model is established using time domain verification. The time domain verification involves comparing the time responses predicted by the model with the responses recorded during flight test. The model was identified for both the hover and medium speed flight condition (10-20 m/sec).

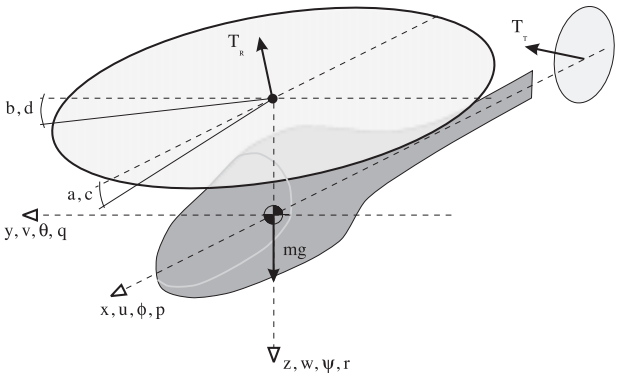

Figure 2 – Helicopter variables with fuselage coordinate system and rotor/stabilizer bar states

Model Structure

The parameterized state-space model is shown in Table 2. The model includes the following states:

$$x = \begin{bmatrix} u & v & p & q & \phi & \theta & a & b & w & r & r_{fb} & c & d \end{bmatrix}^T \quad (1)$$

where (refer to Figure 2 for coordinate axis):

u, v, w are the velocities in the fuselage coordinates

p, q, r the roll, pitch, and yaw angular rates

ϕ, θ, ψ the roll, pitch, and yaw attitude angles about the principal fuselage axis

a, b, (c, d) represent the longitudinal and lateral main rotor (stabilizer bar) flapping angles for a first order tip path plane model

r_{fb} is an additional state used to account for the active yaw damping system

With the exception of the stabilizer bar equations and the active yaw damping system, the model structure presented here is similar to the structure used for full-scale helicopters [6]. However, the R-50 identification results exhibit interesting features: the model has a simple block structure (see Table 2) and has a good

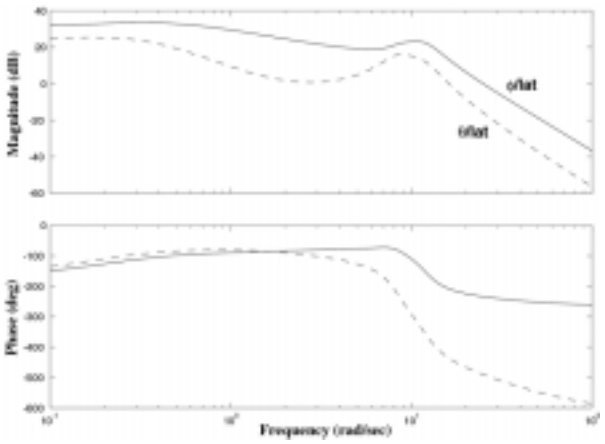

Figure 3 – Roll (solid) and pitch (dashed) response to the lateral input

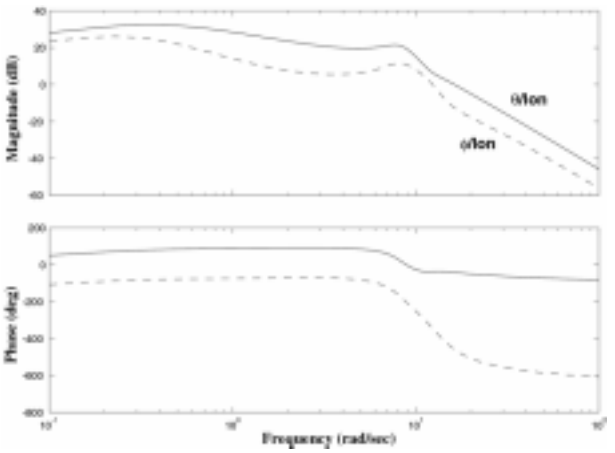

Figure 4 – Pitch (solid) and roll (dashed) response to the longitudinal input

physical consistency (key derivatives such as the rotor and stabilizer time constants agree with the theory); the rotor dynamics affect the vehicle dynamics in a straightforward fashion, which can be explained by the absence of complex aerodynamic effects or rotor fuselage interactions. These features suggest that the model structure we developed could be used as a generic small-scale helicopter model.

In hover conditions, the dynamics of the R-50 are sufficiently decoupled to allow an analysis of the lateral/longitudinal dynamics separately from the yaw/heave dynamics.

Characteristics of the R-50 Attitude Dynamics

Figures 3 and 4 show the frequency responses for the helicopter pitch and roll responses to the lateral and longitudinal cyclic control inputs, respectively. Both attitude responses display a lightly damped second order nature. This is a result of the dynamical coupling between the fuselage and rotor [7]. The lightly damped resonance is due to the presence of a stabilizer bar. The resonant coupled rotor/stabilizer/fuselage r/s/f mode has the following natural frequencies and damping ratio (obtained from the system's eigenvalues):

$$\text{pitch:} \quad \omega = 8.37\,\text{rad/s}, \quad \zeta = 0.20 \qquad (2)$$

$$\text{roll:} \quad \omega = 11.88\,\text{rad/s}, \quad \zeta = 0.22 \qquad (3)$$

From the frequency responses, we see that the off-axis effects of the control inputs are most significant in the lower frequencies and in the region of the coupled r/s/f modes.

Analysis of the Baseline Control System

Description of the Baseline Control System

The control system currently used for Carnegie Mellon's R-50 autonomous helicopter is based on a single-input/single-output (SISO) proportional-derivative (PD) structure. This system provides sufficient controllability and robustness for the maneuvers that are required for slow hover-like flight. A block diagram of the baseline control system is given in Figure 5.

For position control, we use a position loop in cascade with an attitude loop. Two separate systems are used for the lateral and longitudinal systems. The position loop, which uses position and velocity feedback, produces the attitude reference for the attitude loop. The attitude loop uses only attitude angle feedback. The absence of attitude rate feedback is justified by the presence of the stabilizer, which acts as a pseudo rate feedback. The vertical position and the heading are controlled by two separate PD control loops.

Flight Validation of the Baseline Control System

Before proceeding with the analysis and optimization of the baseline control system, we verified how well the model predicts the closed-loop performance Carnegie Mellon's autonomous helicopter. Since a closed loop verification involves all components of the helicopter control system, from the flight-mechanics to the computer systems, it allows us to detect possible

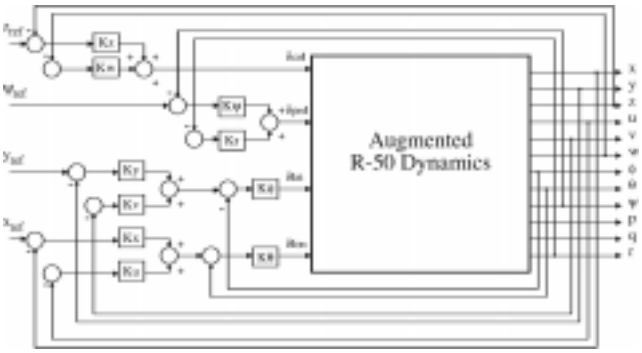

Figure 5 – Block diagram of Baseline Control System

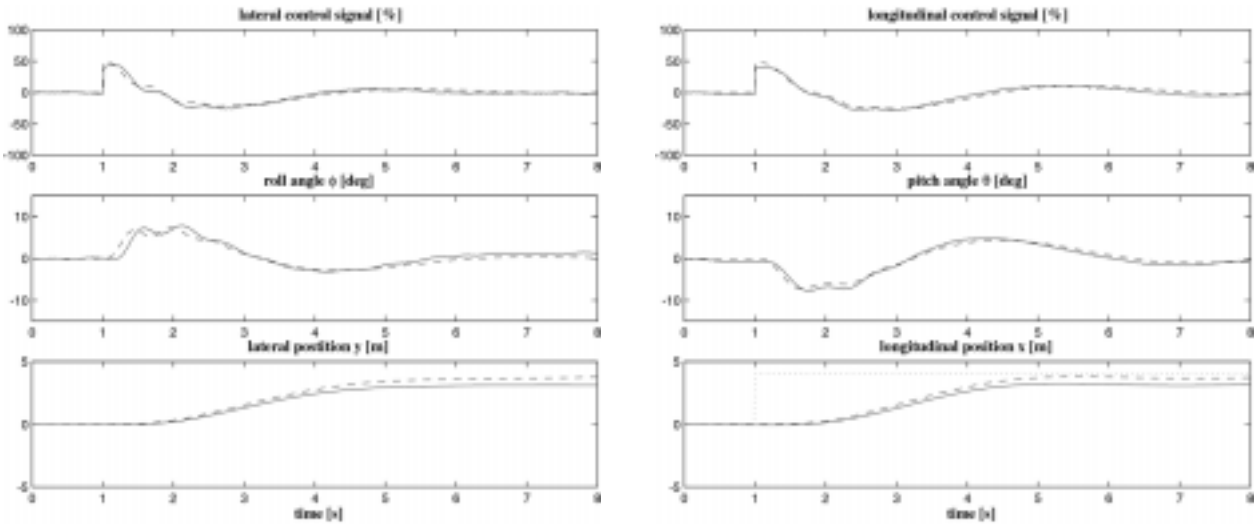

Figure 6 - Comparison between predicted (dashed) and recorded (solid) closed-loop responses for a 4 m step-like position command in the lateral direction (column 1 and 2) and longitudinal direction (column 3 and 4)

anomalies or un-modeled factors.

For the closed loop verification, the helicopter was given a 4-m step-like position reference command individually in the longitudinal (x_{ref}) and lateral directions (y_{ref}). The actual helicopter responses were recorded during the flight-test; meanwhile the predicted helicopter responses were obtained from the model of the closed loop system.

The comparisons between the real and predicted responses, for the lateral and longitudinal directions, are shown in Figure 6. All key variables – the control signals, the attitude angles and the positions – show a good agreement. Notice in particular how the model accurately captures the oscillatory tendency in the attitude angles which is due to the coupled rotor/stabilizer/fuselage dynamics.

Stability Analysis of the Baseline Control System

To determine the performance of the baseline control system, we used gain and phase margins analysis. Figure 7 shows the Bode plots for the lateral and longitudinal loop gain functions with the phase and gain margins indicated.

Compared with the specifications used for flight control design (MIL-F-9490), which require a phase margin of

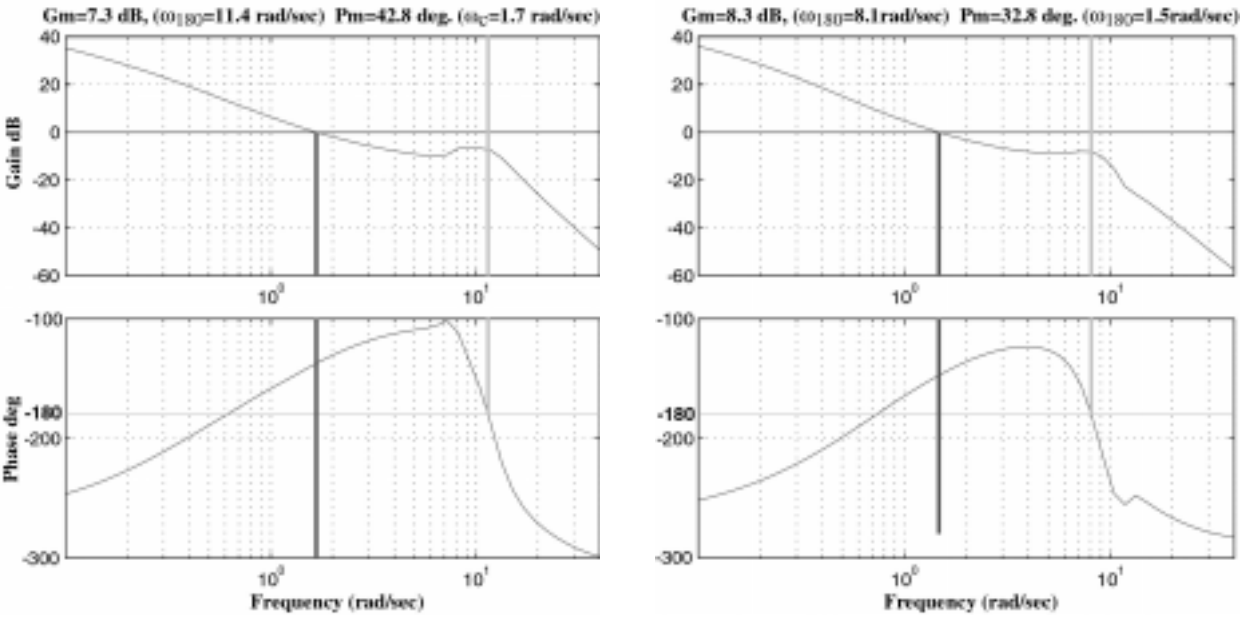

Figure 7 – Bode plot of the loop gain function for the lateral (left) and longitudinal (right) axis showing the phase margin and the gain margin of the baseline control system. Notice that the resonance peak is located precisely at the ω_{180} frequency and thus limits the gain margin

45° and a gain margin of 6dB, the baseline system lacks adequate phase margin. The phase margin can be increased by raising the bandwidth; however, as can be observed from the loop gain function, this would be detrimental for the gain margin. This is a typical situation where the gain and phase margins determine the maximum bandwidth. The bandwidth limitation is particularly pronounced because the critical frequency ($\omega_{180,lat}$=11.4rad/sec and $\omega_{180,lon}$=8.4rad/sec) coincides with the natural frequency of the lightly damped coupled r/s/f mode (Eq. 2-3); therefore, the peak in magnitude of about 14dB ($-\log_{10}(\zeta$=0.2)) translates directly in a reduction in the gain margin. The light damping of the coupled r/s/f mode, caused by the presence of the stabilizer bar, constitutes a performance and robustness limitation for active control.

This analysis shows that the baseline control system already exploits most of the performance available when using attitude feedback. A typical attitude control systems [8] often uses attitude rate feedback; however, with the lightly damped r/s/f mode, the addition of a rate feedback would not be helpful.

Control System Optimization

For the optimization of the attitude control system, the performance limitation resulting from the lightly damped r/s/f, can be addressed using a notch filter, and subsequently by optimizing the control system using the CONDUIT control design environment [3]. In the following only results for the roll axis are presented. The same approach is valid for the pitch axis.

Notch Filter Compensation

By inserting a second order notch filter (Eq. 4) in the attitude control path of the attitude loops (see Figure 9), we can compensate the lightly damped resonance due to the stabilizer bar. Note that this measure does not cancel out the effect of the stabilizer bar but only compensates the effect the stabilizer has on the coupled rotor/fuselage mode. Another solution to the limiting effect of the stabilizer bar would be to physically remove it. This drastic solution, however, would make the helicopter un-flyable by a human pilot in case of a failure.

$$G_{notch}(s) = \frac{s^2+2\zeta\omega s+\omega^2}{s^2+2\omega s+\omega^2} \qquad (4)$$

where ω and ζ are respectively selected to be the natural frequency and damping ratio of the r/s/f mode.

Figure 8, shows the effect of the notch filter, when we choose ω and ζ as the natural frequency and damping ratio of the r/s/f mode (ω_{roll}=11.88 rad/sec and ζ_{roll}=0.22). The resonance peak due to the stabilizer bar is entirely canceled out by the notch filter. With the notch filter, significantly higher attitude gains can be used while providing sufficient gain and phase margin. This allows for a higher bandwidth without exacerbating the r/s/f mode.

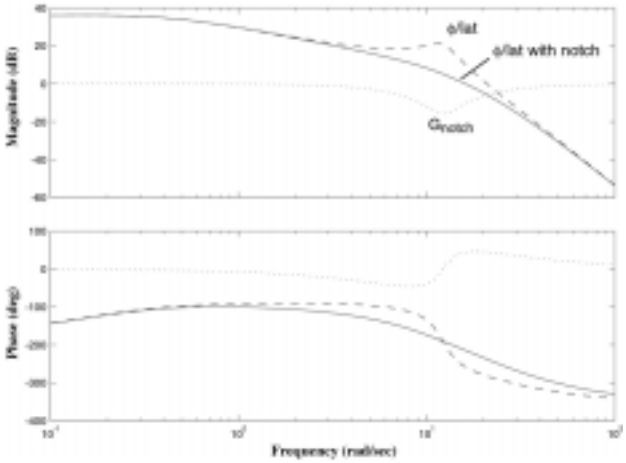

Figure 8 – Comparison between the original roll response (dashed) and the response with the notch filter (solid)

In order for the notch filter to be a practical solution it must be robust to changes in the helicopter configuration, or operational conditions. Hence, we need to understand how the helicopter configuration and operational conditions affect the dynamic characteristics of the r/s/f mode.

For the lateral dynamics, the natural frequency ω_{roll} is a function of the lateral flapping spring L_b [1]:

$$\omega_{roll} \approx \sqrt{L_b} \qquad (5)$$

L_b,is inversely proportional to the roll moment of inertia, which is one of the variables subject to variations. However, a 20 % change of the helicopter moment of inertia, which is a very large variation, only produces a 10 % change in the natural frequency of the r/s/f mode. Shifting the notch filter by ±10 % of the nominal frequency can be tolerated. The damping ratio of the coupled r/s/f mode (ζ_{roll}), is function of the normalized rotor spring coefficient (L_b), and the equivalent rotor time constant [1] (τ_s; for a rotor with stabilizer the effective time constant corresponds to the stabilizer time constant):

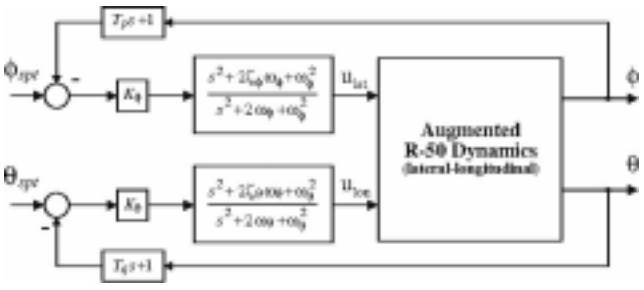

Figure 9 – Block-diagram of the attitude control system

$$\zeta_{roll} \approx 1/(2\tau_s\sqrt{Lb}) \quad (6)$$

The rotor time constant can change with the operating point. However, from our identified model for the cruise flight condition, we noticed less than 10 percent change in the parameters of the r/s/f modes between hover and medium speed cruise flight condition.

Attitude Control Architecture

For the optimization, the baseline architecture was extended by use of attitude rate feedback and a notch filter. The depth of the notch filter was designated to be an optimization parameter to provide more flexibility for the loop shaping. Figure 9 shows the block-diagram of the attitude control system including the notch filter. The optimization parameters are:

K_ϕ, K_θ: lateral and longitudinal attitude gains

T_p, T_q: ratio of rate to angle feedback

$\zeta_\phi,\ \zeta_\theta$: notch filter depth (damping ratio of transfer function zero)

Description of the CONDUIT Design Interface

CONDUIT [3] is an interactive control design framework which integrates the MATLAB environment (e.g. Simulink and other toolboxes) and a powerful multi-criterion optimization engine (CONSOL-OPTCAD). The main advantage of CONDUIT over conventional control design tools or methods is that is allows the optimization of a pre-defined control system architecture against a variety of specifications. The optimization process is supported by statistical and sensitivity tools, which make it possible to determine the sensitivity of the results to the different design parameters as well as possible correlation among the design parameters.

The specifications used by CONDUIT are divided in constraints and performance measure or objectives. The constraints, are typically stability specifications such as eigenvalue locations or phase and gain margins. The performance measures, or objectives, are used to drive the design in a direction that meets the operational requirements. Typical performance specifications include bandwidth, crossover frequency, and damping ratio. Particular specifications can be derived from sources such as handling qualities requirements ADS-33 [9].

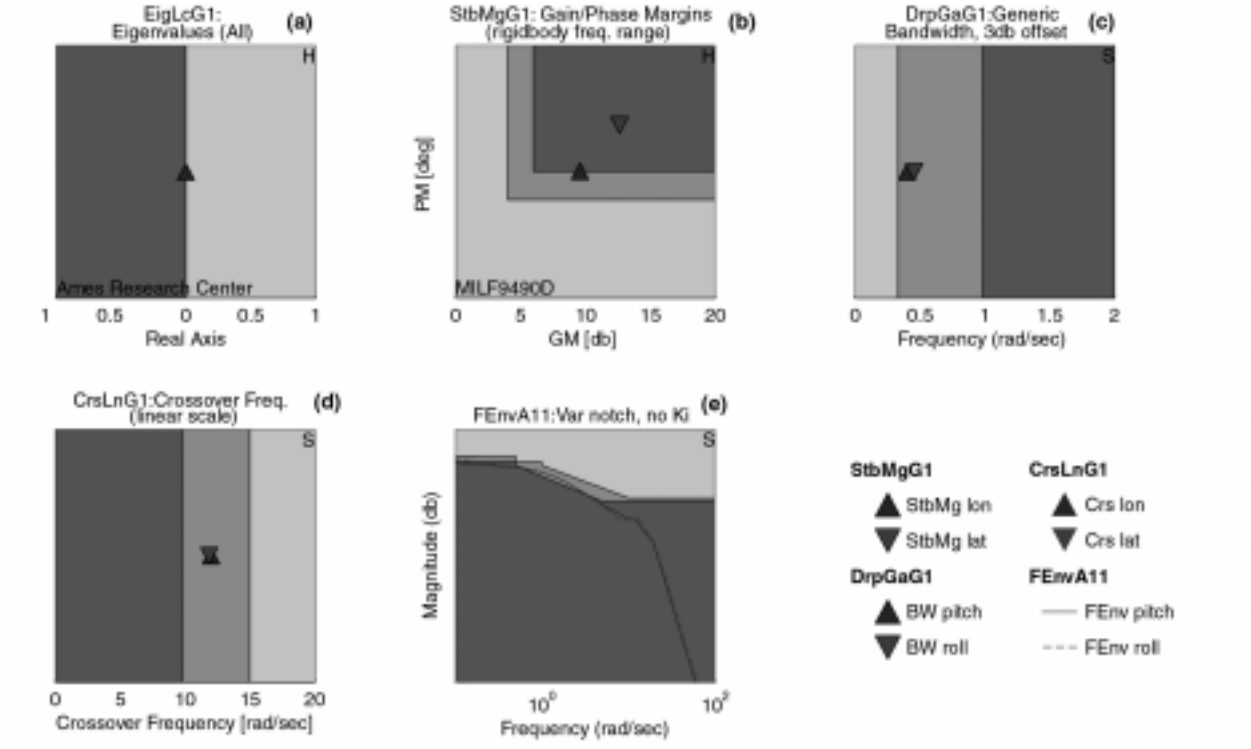

Figure 10 – Specification window showing the specifications used for the optimization of the attitude control system. Notice the frequency envelope specification (e) that was added to the standard CONDUIT specifications. The darker region represents the target range (Level 1)

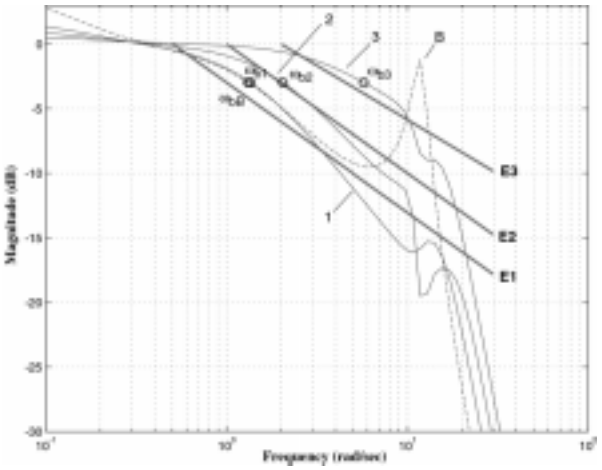

Figure 11 – Comparison between the roll angle frequency responses for different attitude control designs. (B) Baseline system; (1)-(3) Optimized PD system with notch filter in order of increasing bandwidth. Also shown are the Level 1 limits of the frequency response specifications (E1,E2,E3) used for (1)-(3)

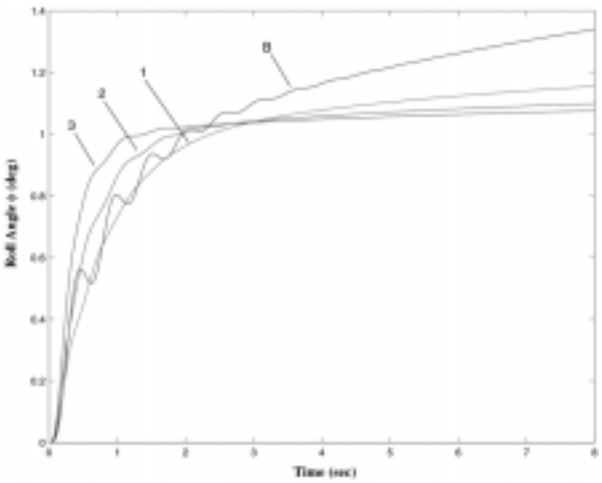

Figure 12 – Comparison between the responses to a roll angle reference step for different attitude control designs. (B) Baseline system; (1)-(3) Optimized PD system with notch filter in order of increasing bandwidth

At each iteration of the optimization, the specifications are evaluated and the result converted into a cost. The cost reflects how far the result is from the target value (or region for the case of two dimensional specifications). Every specification is divided into three levels (1,2,3). Figure 10 shows the specification used for the attitude control optimization. Level 1 (dark gray) represents the target value range, Level 2 (medium gray) represents results with minor to significant deficiencies, and Level 3 (light gray) represents results beyond major deficiencies.

Optimization of the Attitude Control System

The specifications used to optimize the attitude control system for Carnegie Mellon's R-50 are based on elementary attitude control requirements.

Attitude Control Requirements

Since any longitudinal or lateral maneuver of the helicopter is achieved through a change in the helicopter's attitude, the attitude control performance plays an essential role for the overall helicopter performance. The basic attitude control requirements are the following:

- *speed of response*: High bandwidth is necessary for good handling qualities. For full-scale helicopters the specification for a Level 1 handling quality is around 2 rad/sec (ADS-33 [9]). High attitude control bandwidth is also essential for good velocity and position control.
- *sufficient damping of the r/s/f mode*: to limit the short period roll or pitch oscillations.
- *disturbance rejection*: wind gusts act as input disturbances, and therefore high attitude control bandwidth is also beneficial for disturbance rejection.
- *coupling*: since the coupling is most severe in the low frequency range and the frequencies of the r/s/f mode (see Figure 3 and 4), suppressing the r/s/f mode with the notch filter will suppress the high frequency coupling, and high low-frequency gain will address the low-frequency coupling.

Selected CONDUIT Specifications

The CONDUIT specification window used for the attitude control optimization is shown in Figure 10(a)-(e). We selected the following specification:

- *Eigenvalue location* (a): constraints all the real parts of the system eigenvalues to values smaller are equal than zero. This ensures that all the dynamics are stable or neutrally stable.
- *Gain and phase margins* (b): constraint that ensures that a minimum of 45 deg of phase margin and 6 dB of gain margin is satisfied (MIL-F-9490).
- *Bandwidth* (c): performance objective which penalizes small bandwidth of the attitude response. The value specified for the Level 1 are between 0.5 and 4 rad/sec depending on the design.
- *Crossover frequency* (d): performance objective used to limit the crossover frequency. The crossover frequency is a measure of the control activity. The Level 1 limit is set at 10 rad/sec.
- *Frequency response envelope* (e): designed to shape the attitude frequency response. This specification was developed specifically to address the lightly damped r/s/f mode. It will be described next.

In order to precisely influence the characteristics of the attitude response we developed an attitude frequency response envelope. This solution is well suited to limit the oscillations caused by the coupled r/s/f mode, and supports the optimization of the notch filter depth. The specification penalizes an overshoot in the frequency range that is critical for the r/s/f mode.

Figure 11 shows the attitude frequency responses of different designs with three different frequency response envelopes (solid lines designated by the letters E1,E2 and E3, corresponding to least responsive to most responsive). We used the frequency response of the baseline control system (dashed) as guideline for the design of the frequency envelope. The envelope constraints the resonance peak of the r/s/f mode due to the stabilizer bar. By shifting the 0dB frequency of the envelope, different performance levels can be specified.

Optimization Results

We optimized the control system for three different performance levels. Table 3 shows the controller gains. The first column shows the gains for the baseline system (manual tuning, only angular feedback, no notch filter). The other columns correspond to the three optimized systems in order of increasing performance.

Figure 11 shows the frequency responses of these four systems for the roll angle and Figure 12 shows the roll time responses for a roll reference step of 1 degree.

Table 3 - Controller Gains for the baseline system and the optimized systems.

	baseline (B)	slow (1)	medium (2)	fast (3)
K_ϕ	0.04	0.08	0.1267	0.2079
T_p	0	0.4154	0.3236	0.1406
ζ_ϕ	1	0.2241	0.0661	0.1310

The frequency response from the baseline system (curve B in Figure 11) clearly shows the peak due to the lightly damped r/s/f mode. The corresponding time response (curve B in Figure 12) displays the short period oscillation that results from the coupling between the rotor and the fuselage. The optimized control systems with the notch filter using the frequency responses envelope (shown in Figure 11 as the E1,E2,E3 lines) successfully bound the frequency responses peak. Note that the lines represent the Level 1 Limit. All three responses enter slightly the Level 2 region. The frequency response envelopes is also used to specify the desired bandwidth The resulting bandwidth are shown in Figure 11 by circles labeled $\omega_{b1},..,\omega_{b4}$.

The time responses for the roll angle reference step shown in Figure 12 clearly show the improvement in the control performance. The short period oscillation is eliminated and the speed of response reflect the different bandwidth specification. With the notch filter, a significantly faster response was obtained ($\omega_{b1}\cong 1.3\text{rad/sec}$ vs. $\omega_{b4}\cong 6.7\text{rad/sec}$) without exacerbating the coupled r/s/f mode. This increase in performance is obtained by a fivefold higher roll angle feedback gain ($K_{\phi 1}=0.04$ vs. $K_{\phi 4}=0.2079$).

The performance of the attitude control system has significant effects on outer loop control systems such as a velocity or position controller. These effects are visible from the Bode plots of the loop gain functions for the velocity and position with closed attitude control loop.

From the Bode plot of the loop gain function for the lateral velocity (Figure 13), we see that a faster attitude controller provides more phase and gain margin (168 deg for design (3) vs. 125 deg for the baseline system).

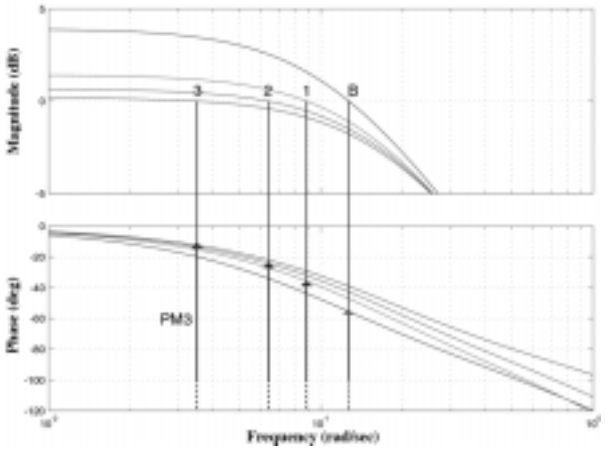

Figure 13 – Comparison of the velocity loop gain function for different attitude control system. (B) Baseline system; (1-3) PD system with notch filter in order of increasing bandwidth. Notice the phase margin increase achieved with faster attitude control (PM3)

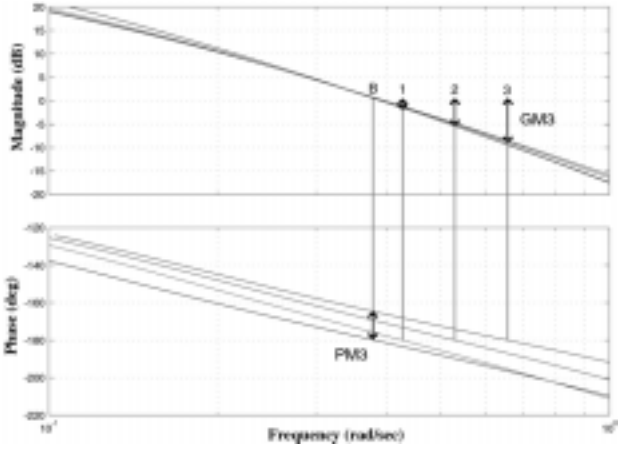

Figure 14 – Comparison of the position loop gain functions for different attitude control system. (B) Baseline system; (1-3) PD system with notch filter in order of increasing bandwidth. Notice the increase in phase and gain margin achieved with faster attitude control (GM3 and PM3)

The increased margin allows for a higher velocity control bandwidth, while maintaining the robustness. The same conclusion can be derived for the position control (Figure 14). For the position control, ω_{180} goes from 0.37 rad/sec to 0.67 rad/sec, resulting in an increase in gain margin from zero to almost 10 dB (Figure 14, GM3). The phase margin for the fastest attitude control design (Figure 14, PM3) is about 15 deg higher than that of the baseline system.

Conclusion

In this paper we have presented control optimization for a small-scale helicopter by using an identified model of the vehicle dynamics that explicitly accounts for the coupled rotor/stabilizer/fuselage (r/s/f) dynamics.

The experiment was performed on Carnegie Mellon's R-50 autonomous helicopter. First we demonstrated the accuracy of the model by showing that it successfully predicts the performance of the currently used control system (baseline controller).

We have shown that the stabilizer bar used in small-scale helicopters decreases the damping of the coupled r/s/f mode. Using elementary stability analysis of the baseline PD controller, we have shown that the lightly damped r/s/f mode limits the bandwidth of the control system. We have then shown that this limitation can be compensated by the introduction of a second order notch filter in the control path.

For the optimization of the attitude controller we have used the CONDUIT control design framework.

The frequency envelop specification precisely specifies the effect of the notch filter and the performance of the attitude controller.

The optimized PD controller with notch filter shows a significant increase in performance and a decrease in the attitude oscillation that resulted from the lightly damped r/s/f mode. Flight test validation will be performed in the near future to confirm the predicted increase in performance.

Acknowledgements

We are very grateful to Dr. O. Amidi, M. DeLouis and R. Miller for the collection of the flight data and for running Carnegie Mellon's autonomous helicopter. This work is also made possible thanks to the support of Yamaha Motor Corporation and funding under NASA Grant NAG 2-1276.

References

[1.] Tischler, M.B. and M.G. Cauffman, "Frequency-Response Method for Rotorcraft System Identification: Flight Application to BO-105 Coupled Rotor/Fuselage Dynamics", *Journal of the American Helicopter Society*, 1992. **37/3**, p. 3-17.

[2.] Mettler, B.F., M.B. Tischler, and T. Kanade, "System Identification Modeling of a Model-Scale Helicopter for the Development of High-Performance Helicopter-Based Unmanned Aerial Vehicles", *Submitted to the Journal of the American Helicopter Society*, 2000.

[3.] Tischler, M.B., et al, "A Multidisciplinary Flight Control Development Environment and Its Application to a Helicopter", in *IEEE Control Systems Magazine*, 1999, p. 22-33.

[4.] Heffley, R.K., "A Compilation and Analysis of Helicopter Handling Qualities Data; Volume I: Data Compilation", 1979, NASA Report CR 3145.

[5.] Prouty, R.W., "Helicopter Performance, Stability and Control", ed. K.P. Company, 1995, Malabar, Fl: Krieger Publishing Company.

[6.] Tomashofski, C.A. and M.B. Tischler, "Flight Test Identification of SH-2G Dynamics in Support of Digital Flight Control System Development. in 55th Forum of the American Helicopter Society", Presented at the *55th Forum of the American Helicopter Society*, 1999, Montreal, Canada.

[7.] Hansen, "Toward a Better Understanding of Helicopter Stability Derivatives", *Journal of the American Helicopter Society*, 1982. 29-1.

[8.] McRuer, D., I. Ashkenas, and D. Graham, "Aircraft Dynamics and Automatic Control", 1973, Princeton, NJ: Princeton University Press.

[9.] Key, D.L., "Handling Qualities Requirements For Military Rotorcrafts", United States Army and Troop Command, 1996, St. Louis, Missouri.